EKSPLOATACJA I NIEZAWODNOŚĆ MAINTENANCE AND RELIABILITY

Eksploatacja i Niezawodnosc – Maintenance and Reliability

Volume 24 (2022), Issue 3

journal homepage: http://www.ein.org.pl

Article citation info:
Bortnowski P, Król R, Ozdoba M. Roller damage detection method based on the measurement of transverse vibrations of the conveyor belt. Eksploatacja i Niezawodnosc – Maintenance and Reliability 2022; 24 (3): 510–521, http://doi.org/10.17531/ein.2022.3.12.

Indexed by: Web of Science Group

Roller damage detection method based on the measurement of transverse vibrations of the conveyor belt

Piotr Bortnowski [a,*], Robert Król [a], Maksymilian Ozdoba [a]

[a] Wroclaw University of Science and Technology, Faculty of Geoengineering, Mining and Geology, Department of Mining, Na Grobli 15, 50–421 Wroclaw, Poland

Highlights

- An original measuring device for transverse vibrations of the conveyor belt was presented.
- The possibility of spectral detection of cooperation of the damaged roller and belt was presented.
- An auto encoder algorithm has been prepared to improve the effectiveness of detection.
- The process of validation of the test procedure under real conditions was conducted.

Abstract

The article presents the detection of damage to rollers based on the transverse vibration signal measured on the conveyor belt. A solution was proposed for a wireless measuring device that moves with the conveyor belt along of the route, which records the signal of transverse vibrations of the belt. In the first place, the research was conducted in laboratory conditions, where a roller with prepared damage was used. Subsequently, the process of validating the adopted test procedure under real conditions was performed. The approach allowed to verify the correctness of the adopted technical assumptions of the measuring device and to assess the reliability of the acquired test results. In addition, an LSTM neural network algorithm was proposed to automate the process of detecting anomalies of the recorded diagnostic signal based on designated time series. The adopted detection algorithm has proven itself in both laboratory and in-situ tests.

Keywords

belt conveyor; conveyor belt; belt vibrations; diagnostics; roller; idler; LSTM; autoencoder.

1. Introduction

The quality of the rollers used, and effective monitoring of their condition is extremely important for the reliable operation of the belt conveyor [29, 32, 36, 57]. Poor technical condition of the rollers may result in the occurrence of mechanical damage to the belt, most often resulting from blocking a single roller in the set [16, 49]. Blockades of the rollers cause excessive friction between the tube and the belt, and consequently accelerated wear, which may lead to a fire focus on the conveyor route [3]. One of the most common causes of roller blockade is bearing damage [1, 55]. In addition, worn bearings significantly increase the resistance to movement, which results in an increase in the demand for electricity [11, 25, 42]. Under operating conditions, roller bearings are exposed to many factors accelerating their wear: dynamic loads, moisture, operating temperature, vibration and dust [43]. Nearly 50% of all conveyor bearing failures are caused by the presence of moisture and dust, which is why the design and quality of the seal is an extremely important factor determining the undisturbed periods of the conveyor [17]. Bearing life is also affected by the lubricants used [12, 35]. Friction between the belt and the blocked roller causes abrasion of the jacket surface until it is destroyed [34]. Local abrasion of the tube also changes the values of dynamic unbalance and radial run-out, the main performance parameters of the rollers [5], which may result in excessive vibrations of the route structure and pose a serious threat of resonance [7]. Damage to rollers very often develops without clear signs, so it is very important to use methods of preventive monitoring of their technical condition [37]. The key indicators assessing the technical condition of rollers during the operation of the rollers are noise levels, vibrations, temperature increases and changes in the properties of the lubricant used [21, 30, 41, 45]. The most used are diagnostic methods using a vibroacoustic signal to evaluate [13, 27, 38, 56]. Algorithms are used consisting in general measurement of the vibration level of bearing nodes, measurement of the peak coefficient, analysis of the signal envelope, surge pulse method, fuzzy logic or wavelet transform [4, 10, 18, 24]. Methods based on the measurement of the vibroacoustic signal are very affordable in the implementation of solutions based on machine learning [33, 52, 53] with high increase of usage in monitoring the operating status of belt conveyors [26, 39]. The second group of methods for assessing the condition of rollers is related to temperature control [32]. The DTS (Distributed Temperature Sensing) method measures the operating temperature of the rollers using optical fiber [51]. Thermal imaging methods are also widely used [9, 34, 47]. Many of the solutions presented require direct installation of measuring devices on the conveyor route or measurements of individual idler sets. In the case of long conveyor routes and hard-to-reach places such as underground

(*) Corresponding author.

E-mail addresses: P. Bortnowski (ORCID: 0000-0002-6647-6234): piotr.bortnowski@pwr.edu.pl, R. Król (ORCID: 0000-0002-2529-1890): robert.krol@pwr.edu.pl, M. Ozdoba, (ORCID: 0000-0002-3364-9442): maksymilian.ozdoba@pwr.edu.pl

mines, these are not optimal solutions, which is why inspection robots [15, 46] or drones [8] are being used more and more commonly. However, there are locations where their use is not possible due to the limited space of the excavation, e.g. narrow drifts with dense construction of the conveyor route or other barriers preventing access to the entire conveyor, such as local changes in the geometry of drift or local accumulations of water. The article proposes a method of detecting damage to rollers based on the transverse vibration signal of a moving, unloaded conveyor belt, measured directly on its surface [6]. A methodology for measuring input signals, filtration and decomposition was proposed to acquire useful data for assessing the state of failure, based on standard frequency analysis. The characteristics of the interference of the signal from the belt are described. A simple LSTM (Long Short-Term Memory) neural network with time memory was built to verify the possibility of detecting damage based on time signals. Tests of the proposed model were conducted on data measured in the laboratory with prepared damage to the roller tube and data measured on the conveyor under mining conditions. The proposed measurement method enables effective detection of the damaged roller and the belt cooperation on sections of routes with difficult access or in the case of long conveyors. Compared to current diagnostic methods, it eliminates the need for additional equipment installed on the conveyor structure and reduces the number of people operating the process. Shortening the measurement time and simplifying the inference process through an autonomous algorithm allows to increase the frequency of diagnostic tests.

2. Materials and methods

2.1. Test rigs

Laboratory tests were conducted on a short conveyor with a length of approx. 8 m, with a 0.8 m wide EP-200 textile belt installed (Fig. 1a). The conveyor was equipped with 5 idler supports (three rollers) with a roller diameter of 133 mm. The average distance between the sets was 0.95 m. The stand allowed for smooth adjustment of the belt speed up to 5.3 m/s. The tests were conducted at 3 selected speeds: 0.4 m/s, 0.9 m/s and 1.3 m/s. The measurement of the linear velocity of the belt and the circumferential velocity of the roller jacket was performed by the installed incremental encoders. Speed control allowed to control a change in the characteristic frequency of the damaged roller [14]. Because the transverse vibrations of the belt depend on the tensile force, a constant tensioning force was provided at the level of approx. 2 kN [6]. The measurement of the tensioning force was made possible by strain gauges installed on the stand.

Field tests were conducted on the PT-1000/60 conveyor with a length of 78 m and an angle of inclination of 16°, used to transport aggregate in a granite mine (Fig. 1b). On the conveyor was installed textile belt Z4P - 630 - 1- I - 1000 [19]. The diameter of the roller tube in the troughed support was also 133 mm. The tests were conducted only at the nominal belt speed, i.e. 1.81 m/s because the conveyor was not equipped with a speed control system. The pre-tension of the belt was caused by a gravity take-up device, at the level of approx. 10.5 kN.

To simulate the damage on the laboratory conveyor, a 133 mm diameter roller with point damage on the surface of the steel tube was used (Fig. 2). The damage is designed to correspond to characteristic tube defects under real operating conditions [31], where abrasive wear of the steel surface arises due to excessive friction with the belt and the process is accelerated by the presence of abrasive materials. The form of damage simulates the local loss of the steel surface and the characteristic sharp edges, which in laboratory conditions affect the change in the geometry of the tube and force the belt to vibrate.

Fig. 2. Prepared point damage to the test roller tube

2.2. Methodology

In the research, original measuring device enclosed in a sealed housing and fixed to an unloaded belt was used (Fig. 3). This approach allowed to eliminate the occurrence of inertial movements caused by vibrations of the belt itself. The device moved from the return pulley to the drive pulley, recording vibration signals along the entire length of the route.

2.3. Characteristics of the measuring device

The most important element of the measuring device is a microcontroller that performs the acquisition of measurement data from the vibration sensor, their initial processing, and data recording on the SD card. The system is equipped with a battery power supply. An analog accelerometer was used to measure the acceleration of vibrations in the vertical direction. The accelerometer allows the measurement of

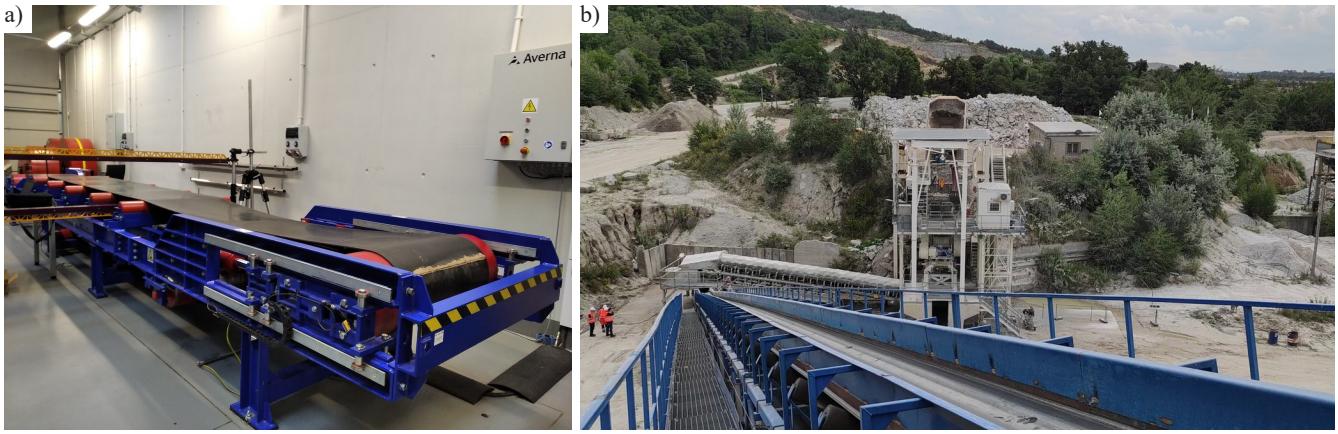

Fig. 1. Measuring stations: a) laboratory conveyor, b) PT-1000/60 conveyor in aggregate mine

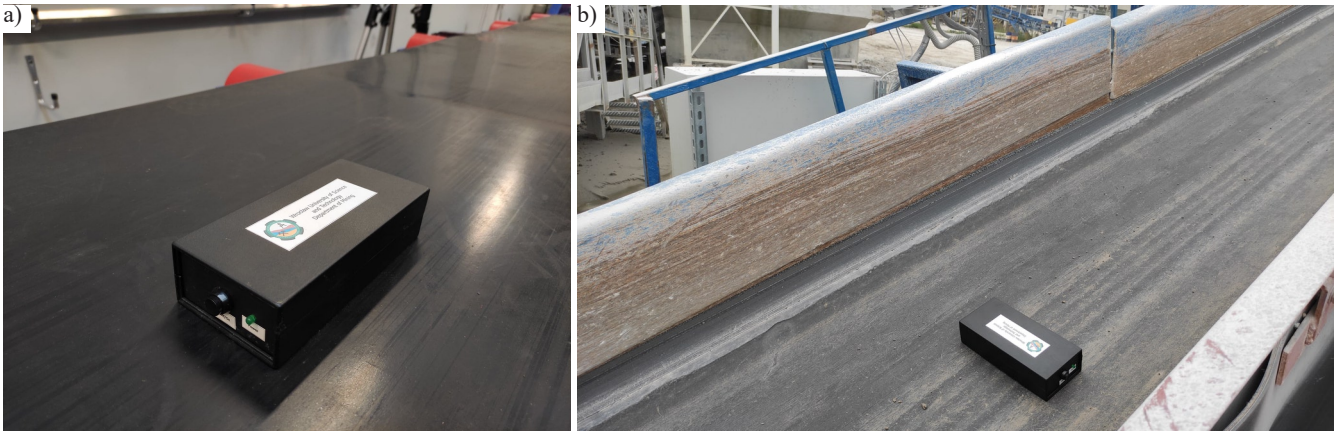

Fig. 3. Measuring device: a) located on the laboratory conveyor belt, b) on the PT-1000/60 conveyor

the vibration signal in 3 axes, but because the belt vibration signals are dominated by transverse vibrations, it was decided to simplify the analysis of the results and measure only the vertical component [22]. The stabilization of the supply voltage was solved by adding a converter to the system. The output signal is monitored for free-fall signal detection to eliminate signals that may be caused by contact-loss of the measuring device from the belt, e.g., due to faulty mounting. The device allows you to sample the signal at a frequency of 2500 Hz. This means the possibility of recording the frequency of characteristic failures up to 1250 Hz. The presented method is dedicated to detecting damage to the surface of the roller tube, unbalance of the rollers and radial run-out due to poor roller quality or bearing degradation. All these factors affect the quality of the roller – belt contact. These are damages with low characteristic frequencies, causing vibrations of the belt of significant amplitude.

Acquiring the correct absolute value of the measured vibration accelerations required a preliminary calibration of the accelerometer. Calibration allows to acquire a precise value of vibration acceleration in relation to the analyzed system. It was conducted through the installation of the measuring device in a state of equilibrium, isolation of the system from all external vibrations and long-term measurement of the indications of analog outputs of the sensor. The measured signal during the measurements was reduced by the average value acquired during calibration. Based on the known measurement resolution of the microcontroller and the sensitivity of the sensor, the voltage signal was transformed into the result in acceleration units.

3. Results

3.1. Frequency analysis

Figure 4 demonstrates examples of time signals acquired for a conveyor during its normal operation and a conveyor with simulated, point damage to the roller tube. This chapter details the data processing for one recorded speed of 0.9 m/s. The length of the recorded signal is in relation to the speed of the belt. In the time-frequency analysis, a characteristic algorithm for detecting local damage to rotating elements was used [54]. The main objective of the analysis was to determine the presence of frequencies characteristic damage in the signal, cyclicity and distribution of frequency changes dominant during the conveyor operation with damage in relation to the distribution for normal operating conditions.

A clear signal was acquired, generated by the forced damage to the roller. The discussed case of roller damage detection in laboratory conditions is a simple issue, because for effective detection it is enough to use classic diagnostic models based on changes in the vibration amplitude. However, such an approach is not possible in the case of the analysis of signals recorded on a mine conveyor, which is discussed later in the article. At this stage, the focus was on the possibility of detecting the characteristic frequencies in the belt signal, the description of the cyclical nature of the recorded phenomena and the influence of the belt damping properties and environmental disturbances on the acquired results. Measurement of vibration acceleration by means of electronic accelerometers in mechanical systems is burdened with noise and disturbances, as a result of the action of acoustic vibrations [48]. In order to reduce the interference, a three-stage input signal filtering algorithm was used. Due to the wave nature of the damage

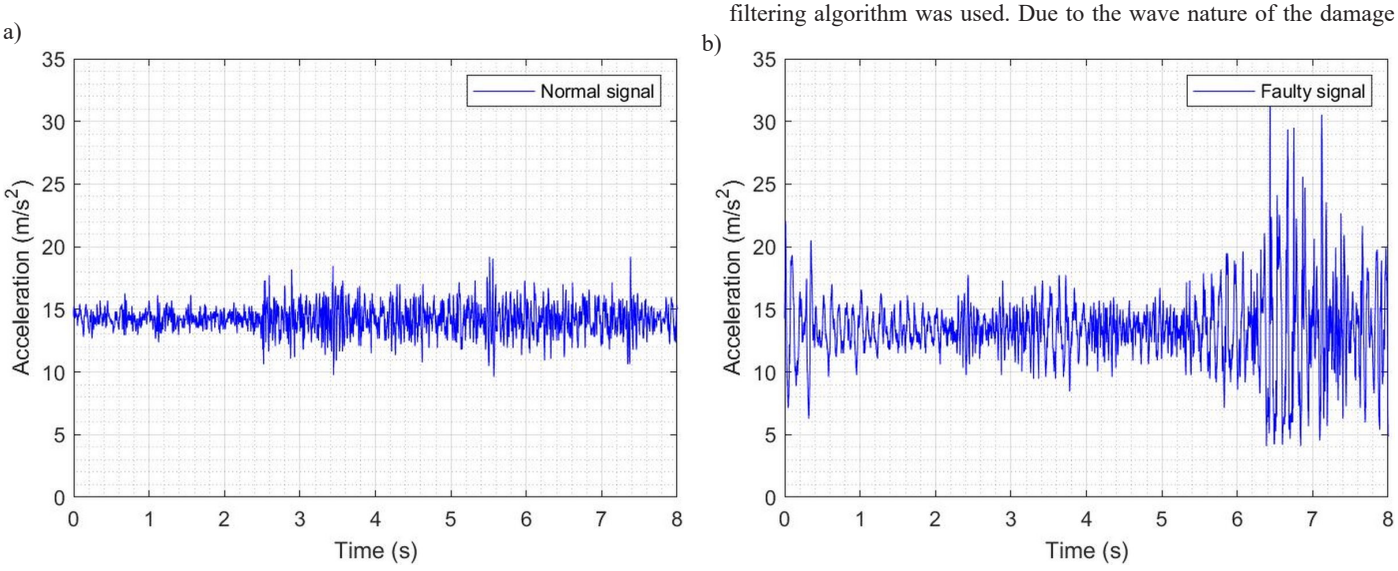

Fig. 4. Acceleration of transverse vibrations along the length of the laboratory conveyor: a) without damaged roller, b) with damaged roller

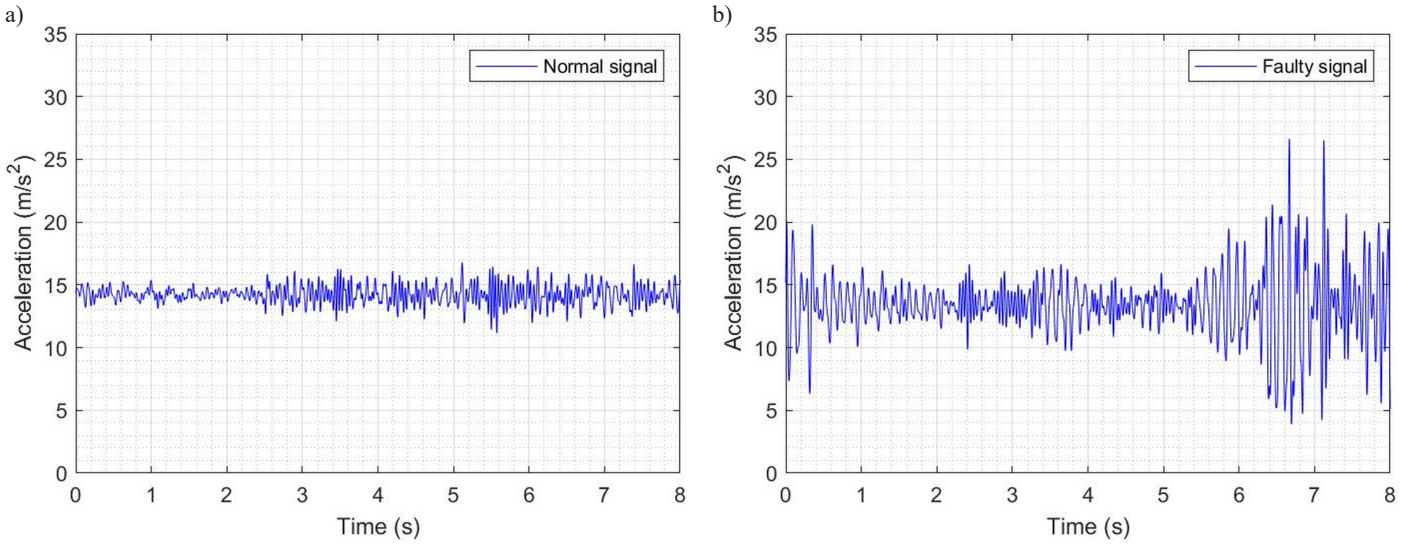

Fig. 5. Acceleration of transverse vibrations along the length of the laboratory conveyor after filtration: a) without a damaged roller, b) without a damaged roller

signal, filtering with wavelet decomposition was used first [44, 58]. Then, a one-dimensional median filter was used, which allows for effective elimination of point interference, and at the same time does not cause distortion of the slopes [59]. The last stage of filtration was the use of a Butterworth low-pass filter to eliminate high-frequency interference characteristic of electronic accelerometers [60]. The filter parameters were selected on the basis of the spectral analysis of the input signal (signal density and the range of the read interferences). Figure 5 presents the time signals after decomposition and filtration, which were used for further frequency analysis.

The damage is located in the last segment of the input signal, therefore the last signal fragment with a duration of 3 s was separated for further processing. Figure 6 demonstrate spectrograms (SPC), time-frequency characteristics of the normal and faulty signals. For this purpose, the short-time Fourier transform (STFT) was used, which in the continuous domain is represented by the equation [28]:

$$STFT\{x(t)\} = X(\tau,\omega) = \int_{-\infty}^{\infty} x(t)w(t-\tau)e^{-i\omega t}dt \tag{1}$$

where: $w(t)$ – window function, $x(t)$ – transformed time signal, ω – frequency.

The discrete form of the STFT for splitting a time signal into overlapping data frames has the form [28]:

$$STFT\{x[n]\}(m,\omega) = X(m,\omega) = \sum_{n=-\infty}^{\infty} x[n]w[n-m]e^{-j\omega n} \tag{2}$$

where: $x[n]$ – signal, $w[n]$ – an analysis window that is assumed to be non-zero only in the range $[0, N-1]$.

$$X(n,k) = X(n,\omega)\big|_{\omega=\frac{2\pi}{N}k} = \sum_{m=-\infty}^{\infty} x[m]w[n-m]e^{-j\frac{2\pi}{N}km} \tag{3}$$

For the above conditions, the spectrogram representation can be declared as:

$$SPC\{x(t)\}(\tau,\omega) \equiv |X(\tau,\omega)|^2 \tag{4}$$

The SPC (Fig. 6) is presented considering the significant frequency range up to 100 Hz.

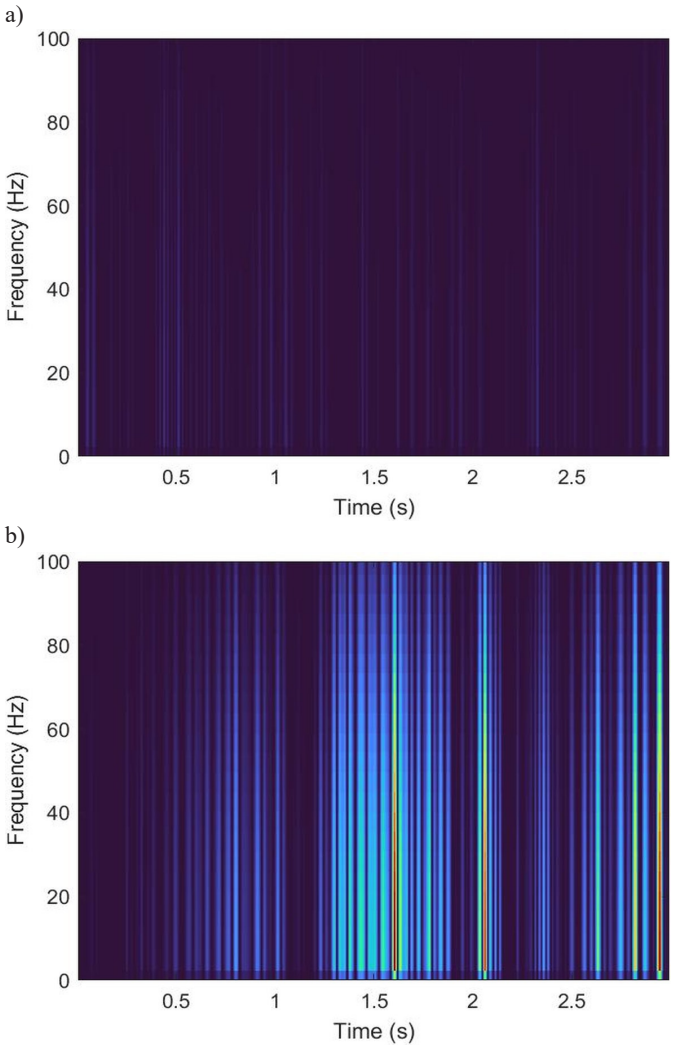

Fig. 6. Transverse vibration spectrogram of the time segment with the identified damage after filtration: a) normal signal, b) faulty signal

At this stage of the analysis, low-frequency damage signals are characteristic for the point damage of the roller tube, which is a slow-rotating element. Visible are cyclical pulses from the damaged roller, with a large amplitude compared to the normal signal. In order to confirm the cyclical nature of the events coming from the roller rotation, the signal autocorrelation (ACF) will be performed in the next step. The autocorrelation function makes it possible to exclude the random-

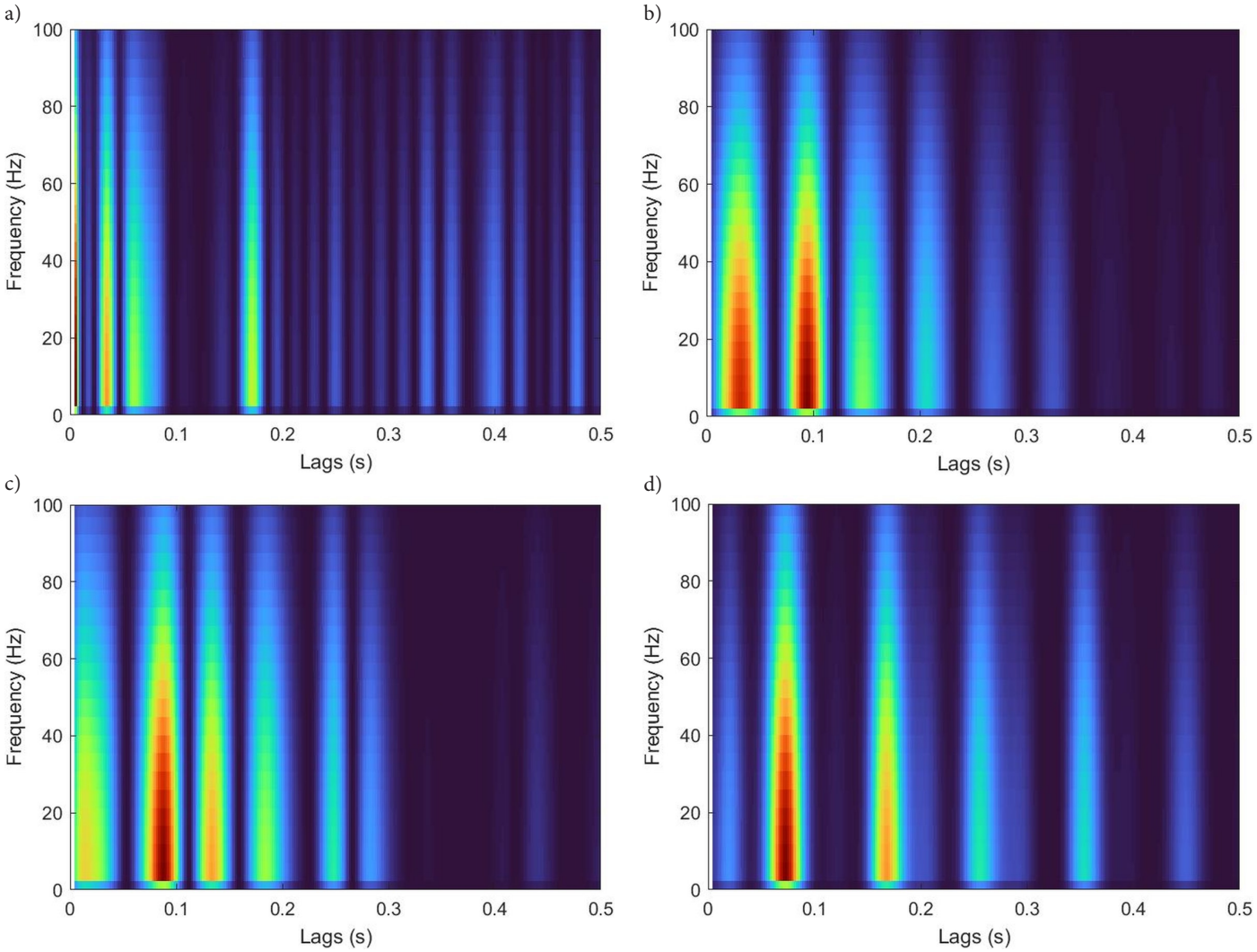

Fig. 7. Spectral autocorrelation of transverse vibrations of time segments with a localized test roller: a) for the roller without damage (normal signal), b) for roller damaged at 0.4 m/s, c) for roller damaged at 0.9 m/s, d) for roller damaged at 1.3 m/s

ness of the signal (it determines its origin from the non-random factor, which in this case is the mantle damage) and to determine the cycle length. Autocorrelation for continuous signals is defined as [23]:

$$ACF(\tau) = \int_{-\infty}^{\infty} x(t+\tau)\overline{x(t)}dt = \int_{-\infty}^{\infty} x(t)\overline{x(t-\tau)}dt \tag{5}$$

where: τ – lag, $\overline{x(t)}$ – complex conjugate $x(t)$.

The ACF for a discrete signal is: [23]:

$$ACF(\xi) = \sum_{n\in Z} x(n)x(n-\xi) \tag{6}$$

where: ξ – lag.

Figure 7 demonstrates the normalized spectral autocorrelation of the normal and damaged signals for the analyzed speed variants. Normalization was performed on the basis of the mean. The plots were prepared for a lag of 0.5 s

From the acquired spectral autocorrelation plots, the disturbances and the result for the zero lag were filtered out, when for obvious reasons the autocorrelation value was equal to one. The ACF of the fault signal indicates a clear maximum (not visible with the ACF of the normal signal), with a lag of approximately 0.1 s, which translates into a fault frequency of 10 Hz. The acquired result is consistent with the analysis of the periodicity of the maximum amplitudes presented after filtration in Figure 5. Detailed analysis reveals a slight increase in the failure frequency with increasing speed from 9 Hz for a speed of 0.4 m/s to 10.2 Hz for a speed of 1.3 m/s. ACFs have one distinct common component with a lag of approximately 0.18 s (5.6 Hz). The best results were acquired for the highest belt speed, which is due to the limited impact of broadband high-frequency interference.

Because the SPC of the normal and faulty signal (Fig. 6) are quite different, the characteristic features of the signal can be distinguished and used to determine changes in the frequency domain associated with the appearance of point tube damage. Mean peak frequencies (mPF) were used as an indicator of the condition of the roller. In the case of describing the spectrogram as a function of two variables $P(t,\omega)$, the peak frequency (PF) can be defined as [61]:

$$PF(t) = argmax_{\omega} P(t,\omega) \tag{7}$$

On the other hand, the mean peak frequency is described by the relation [61]:

$$mPF = \frac{1}{T}\int_0^T PF(t)dt \tag{8}$$

The segmentation function was used to divide the signals into 13 smaller segments. The number of samples in each segment determines

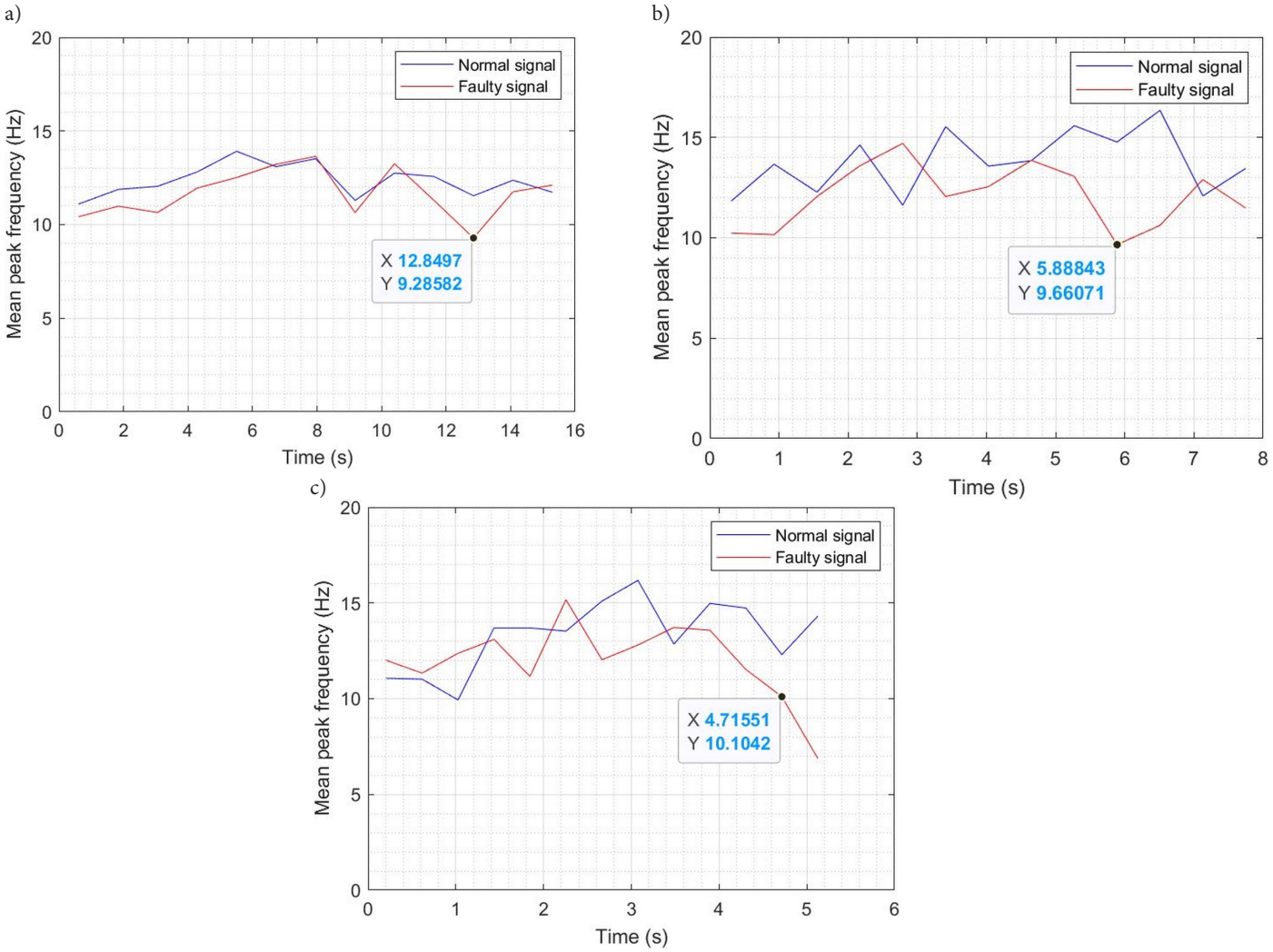

Fig. 8. Change of the mean peak frequency during the movement of the device from the return pulley to the drive pulley: a) for a speed of 0.4 m/s, b) for a speed of 0.9 m/s, c) for a speed of 1.3 m/s

the total number of signal samples (the higher the tested speed was, the smaller the number of samples in the segment). Determined mPF for each segment. Figure 8 demonstrates the changes in the mPF of the normal and faulty signal during the movement of the measuring device on the laboratory conveyor from the return pulley to the drive pulley, for all analyzed speed variants. The test roller location point was also marked to identify mPF changes in this segment.

Figure 8 demonstrates the change in mPF at the location of the test roller between the normal signal and the damage test signal. The slight differences between the results acquired on the basis of the ACF result from the inaccuracy of the segmentation grid. The limitations of the diagnostic method, consisting in the assessment of mPF changes during the operation of the conveyor along the route, are low-frequency environmental signals of the conveyor's operation, which should not be interpreted as a source of potential damage.

In the case of mine conveyors, changes in the mPF in the range of low frequencies (characteristic for damage to the surface of rollers) may be unclear, and the standard diagnostic method of rotating elements, based on the above assumptions, may not be practical. The analysis presents, that point changes in the peak value of the vibration amplitude bring much more valuable information. An automated detection system based on a manually defined alarm threshold of exceeding the permissible peak amplitude value may generate erroneous alarm signals. The result of this state is a dynamic load on the belt due to a randomly changing stream of bulk material [20]. The solution to reduce future errors are autoencoder algorithms, which enable the reconstruction of the signal based on the known characteristics of the device operation under normal conditions.

3.2. Autoencoder application

Automation of the time signal anomaly detection process, based on changes in the peak value of the vibration amplitude, was based on the LSTM autoencoder model, an artificial, recurrent neural network (RNN) [50]. LSTM uses deep learning to reconstruct nonlinear time series. The basis of the system's operation is a signal defined as the normal operating state, which the embedded neural network learns. On this basis, anomaly points in the reconstructed signal can be identified [40]. The idea of the autoencoder operation is presented in Figure 9.

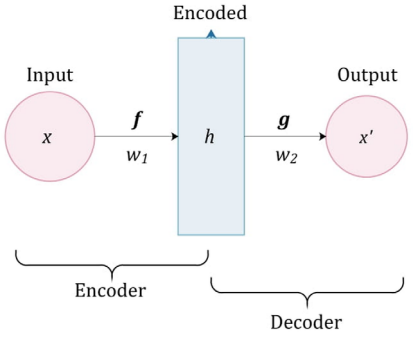

Fig. 9. Diagram of autoencoder operation for discrete time series anomaly detection [2]

The general equations of the autoencoder is presented in the figure above take the form [2]:

$$h = f(x) = \sigma_1\left(W^{(1)}x + b^{(1)}\right) \tag{9}$$

$$x' = g(h) = \sigma_2\left(W^{(2)}h + b^{(2)}\right) \tag{10}$$

where: f – encoder function, g – decoder function, $g \circ f(x)$ – reconstructed input x, h – the encoded representation of the input x, σ_1, σ_2 – activation functions, $W^{(1)}$, $W^{(2)}$ – weight matrices, $b^{(1)}$, $b^{(2)}$ – bias vectors.

The autoencoder loss function to minimize the reconstruction error is defined as [2]:

$$L(x,x') = \|x - x'\|^2 = \| x - \sigma_2(W^{(2)}\left(\sigma_1\left(W^{(1)}x + b^{(1)}\right)\right) + b^{(2)} \|^2 \tag{11}$$

The diagram of the neural network used is demonstrated in Figure 10.

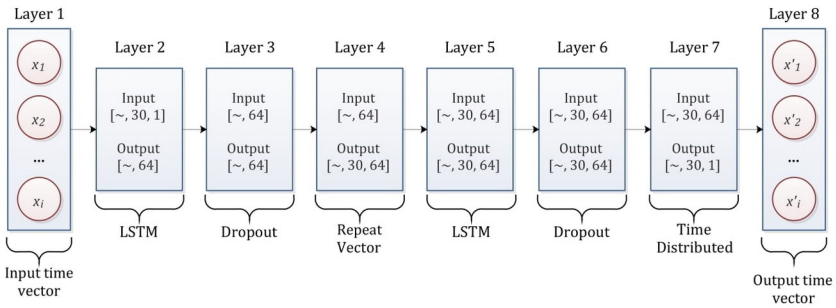

Fig. 10. Scheme of the application of the neural network

Layer 3 and layer 6 are responsible for the regularization of the data in order to overfitting the model and improve its efficiency. Layer 4 repeats the input vector according to the defined number of backward time steps. For the model, this parameter was set to 30 samples. Finally, layer 7 creates a time vector with a length equal to the number of outputs from the previous layer. As the loss index, the mean absolute error (MAE) was used, defined as:

$$MAE = \frac{1}{n}\sum_{i=1}^{n}|x_i - x'_i| \tag{12}$$

where: n – number of data points, x – actual value, x' – value predicted by the model used.

3.2.1. Laboratory conveyor

In the case of laboratory tests, the signals of the normal operation of the conveyor (Fig. 11) were defined for the work with the roller in good technical condition (recorded before the damage was prepared).

Figure 12 demonstrates the model losses acquired during successive iterations for training and test data at a speed of 0.9 m/s.

The places where the test loss (faulty signal) is lower than the training loss (normal signal) may mean that the failure variant considered by the model was trivial to predict, significantly different from the data defined as the normal state. This situation is illustrated in Figure 4 as the signal peaks at the location of the damaged roller. The next figure (Fig. 13) demonstrates the MAE distribution for training

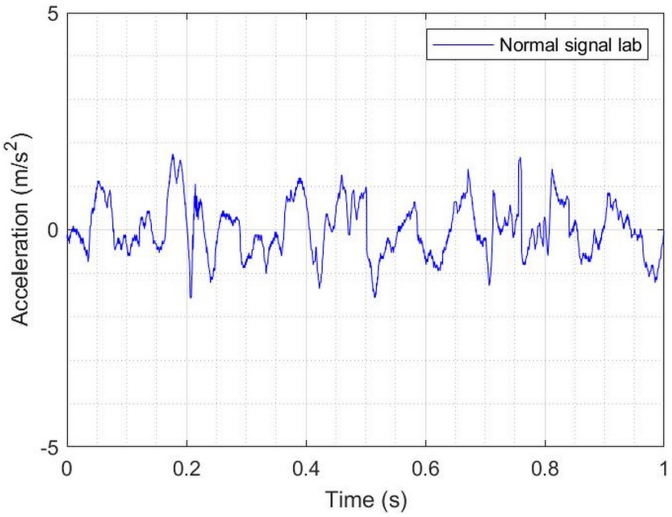

Fig. 11. A slice of the scaled time signal (without damage) for training the neural network

and test data. The red line presents the course of the expected normal distribution.

The learned algorithm was used to predict anomalies in the signal from the laboratory conveyor (Fig. 14). For the purposes of these studies, the thresholding parameter was defined as the maximum value of the vibration magnitude of the normal signal.

3.2.2. PT-1000/60 conveyor

For a conveyor operated in real conditions, the normal signal was assumed as a time slice with a standardized distribution with respect to other segments. Figure 15 demonstrates short time slices of signals used to train the neural network.

Figure 16 presents the acquired model losses during successive iterations for the training and test data recorded on the conveyor in full scale.

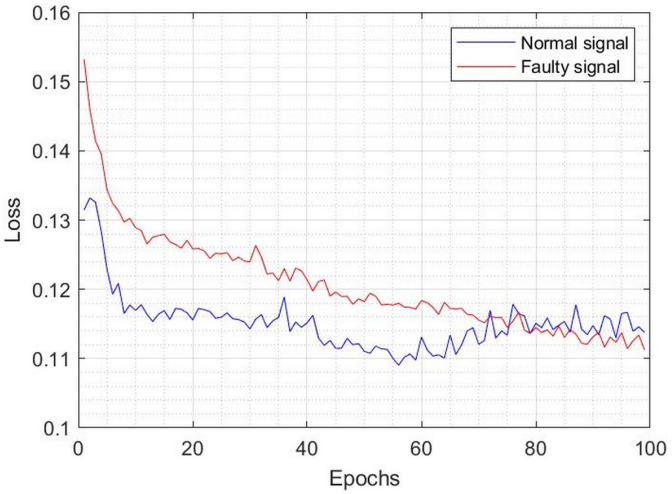

Fig. 12. Model learning loss for successive iterations

In this case, a potentially faulty signal is the signal collected during the full travel of the device on the route, from the return pulley to the drive pulley. Over the entire length of the route, there were over 90 idler supports, which were verified.

As in the case of laboratory tests, Figure 17 demonstrates the distribution of MAE for the normal signal and the complete signal recorded on the conveyor.

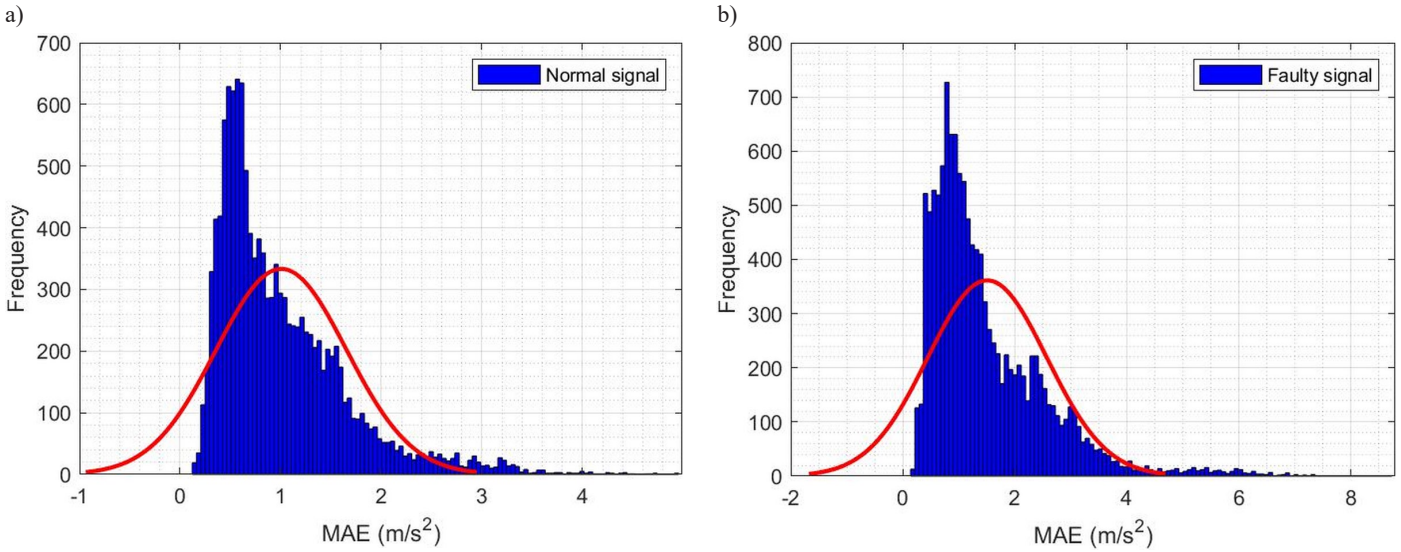

Fig. 13. MAE histogram with the determined normal distribution: a) for training data (normal), b) for test data (faulty)

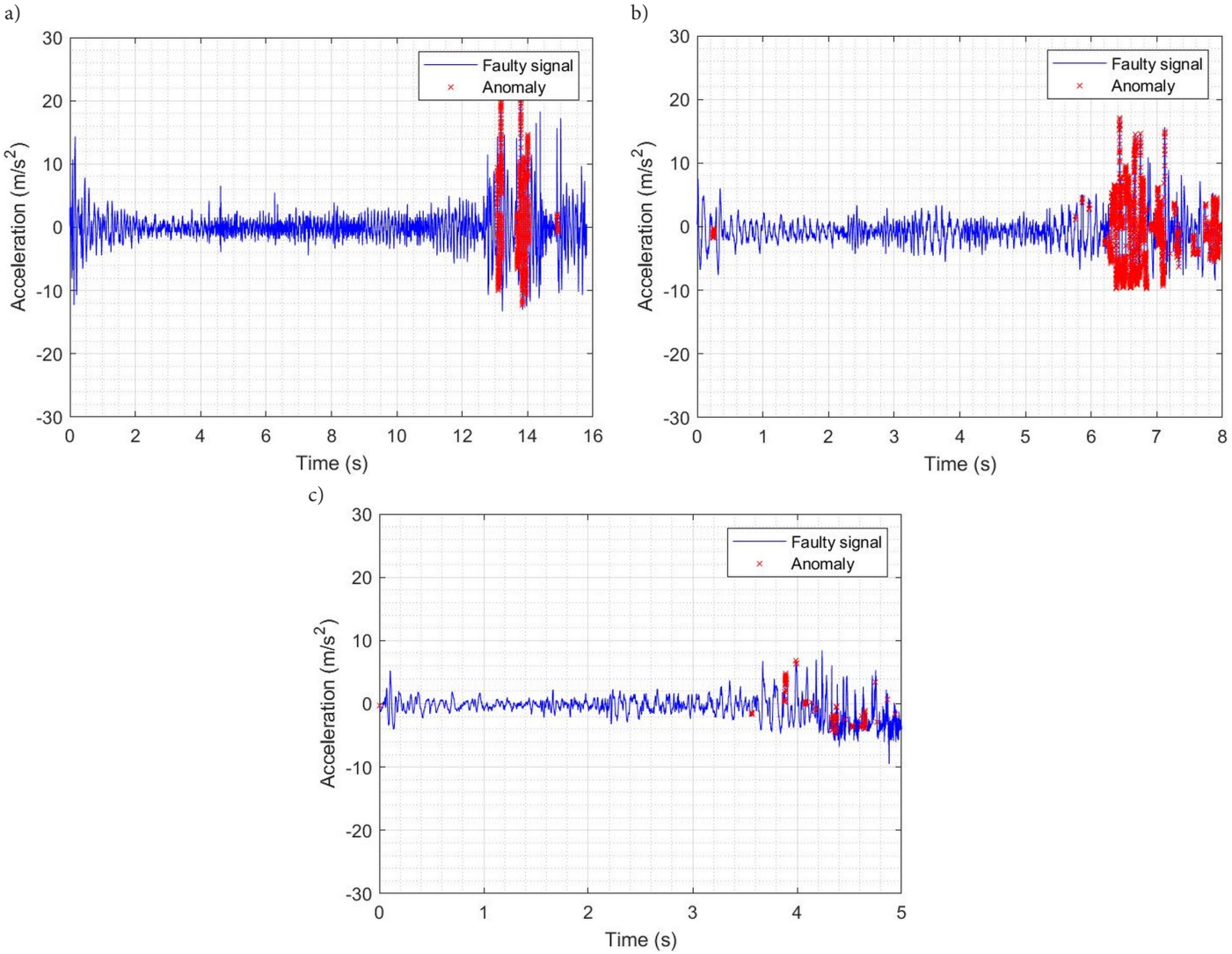

Fig. 14. Detection of anomalies in a scaled laboratory signal: a) for a speed of 0.4 m/s, b) for a speed of 0.9 m/s, c) for a speed of 1.3 m/s

The results of roller anomaly detection with the use of the autoencoder are demonstrated in Figure 18, and the on-site inspection confirmed the place of their occurrence in the indicated sections of its route.

In the recorded signal, the autoencoder detected 3 locations of potential damage to the roller. The first point of damage was found at the point of loading the material onto the conveyor, at the very beginning of the route (approx. 2 seconds). The registered signal anomalies were caused by damage to the roller bearing (Fig. 19a), which lost its functional properties due to damage to the seal or degradation of the

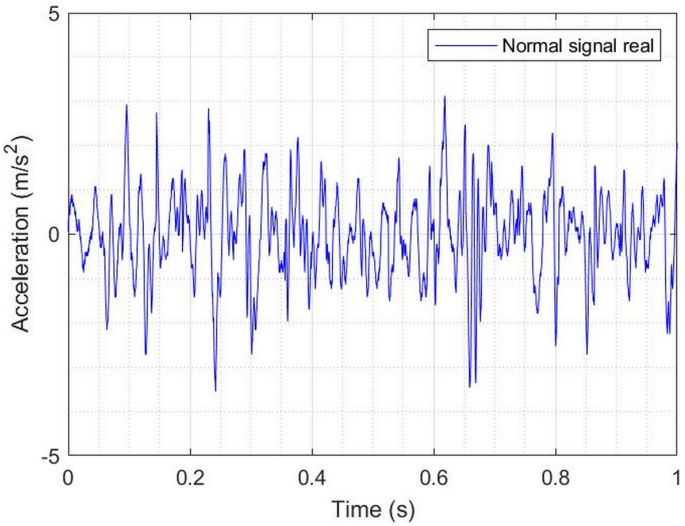

Fig. 15. A slice of the scaled time signal (without damage) for training the network

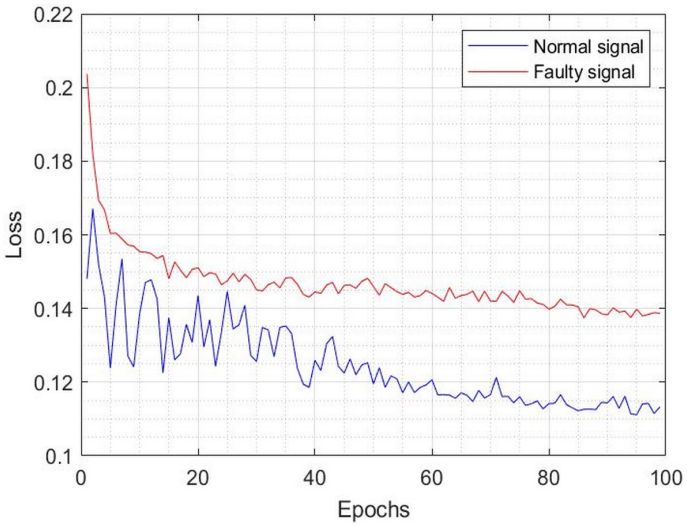

Fig. 16. Model learning loss for successive iterations

a)

b)

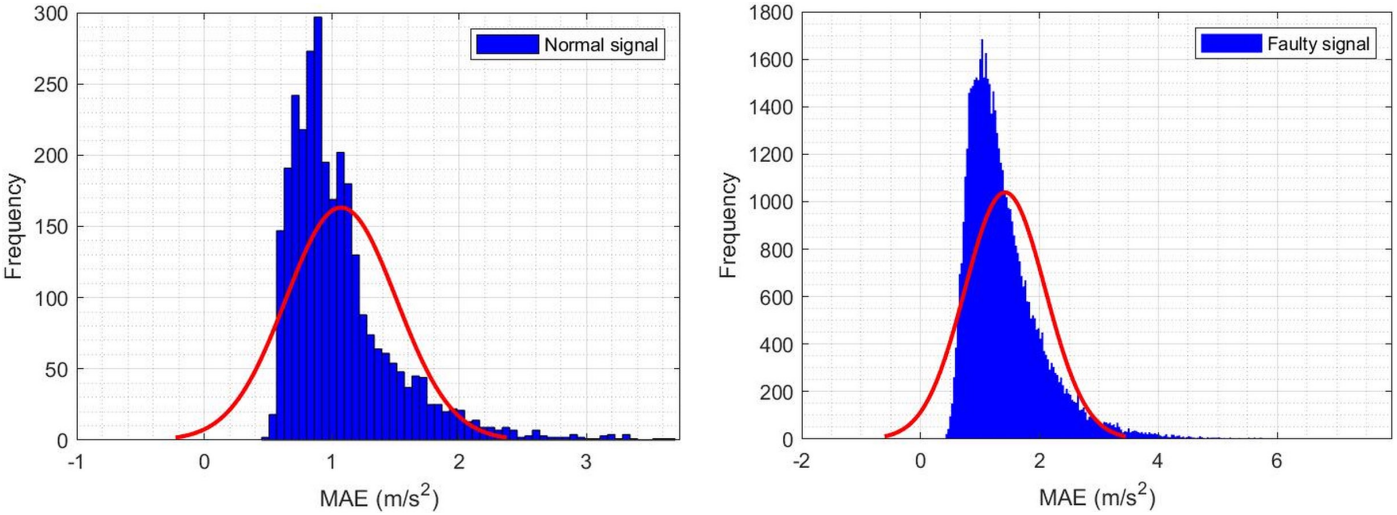

Fig. 17. MAE histogram with determined normal distribution: a) for training data (normal), b) for test data (potentially faulty)

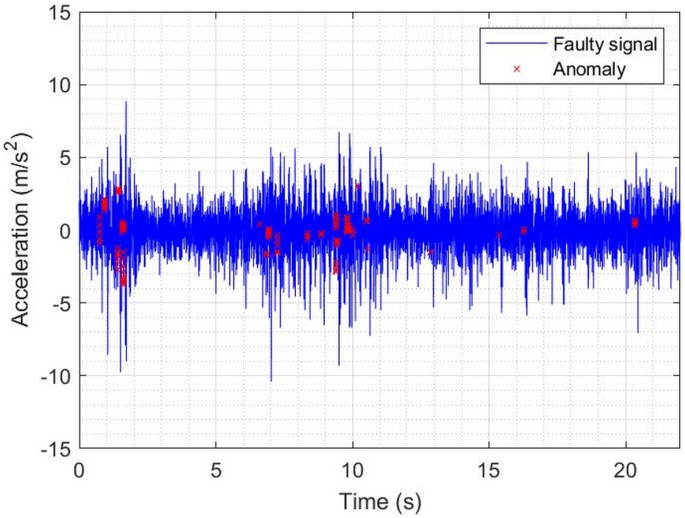

Fig. 18. Anomalies were detected in the transverse vibration signal of the full-scale conveyor

joint between the rollers tube and the hub. The work of this particular roller was much louder than the other rollers in the same set. The second point of damage (approx. 7 seconds) was related to the friction of the belt against the blocked tracking roller (Fig. 19b). The third point of damage (approx. 10 seconds) was caused by abrasion of the roller tube (Fig. 19c), which was replaced immediately after the tests.

4. Summary and conclusions

The article presents a method of roller diagnostics based on analysis of recorded signal of transverse vibrations using a measuring device located on the surface of the belt. The research was conducted in laboratory conditions with prepared damage to the roller tube, in a known location along the route, and then the process of validating the adopted test procedure in real conditions was performed. The recorded vibration signals were filtered and decomposed to reduce noise, and then subjected to standard frequency analysis. There were differences in the measurement results acquired for signals recorded in the presence of a damaged element and in the normal state (without damage), which were characterized by different values of signal amplitude.

Studies have proven that for laboratory conditions it is possible to find the location of the damaged element based on the change in the average peak frequency over time and spectral autocorrelation. The use of spectral autocorrelation proved the cyclicity of the signal in the case of a damaged roller and allowed to indicate its frequencies of excited vibrations.

The limitation of the use of the diagnostic method, consisting in the assessment of mPF changes during conveyor operation in real conditions, are numerous, low-frequency signals related to the specificity of the operating conditions, which can be mistakenly treated as

Fig. 19. Anomalies found on the belt conveyor route: a) damaged roller bearing, b) blocked belt tracking roller, c) damaged roller tube

a source of potential damage, but in fact are only signal interference. This prompted the authors to develop an autoencoder model that required building an LSTM neural network algorithm with time memory, where damage detection is based on a comparison of recorded time signals with a signal used for deep learning and corresponding to normal operating conditions. The adopted detection algorithm effectively located the damaged roller at the laboratory stand and indicated potential areas of existing or developing damage to the rollers built on the mine conveyor, which was confirmed by the local inspection of the facility. The use of the auto encoder also resulted in the automation of the damage detection process, which can be extremely valuable when assessing the operation of long-distance conveyor routes. The proposed system of non-invasive diagnostics of the cooperation of the conveyor belt with the roller, as well as the presented method of interpretation of the recorded signals is characterized by high application potential. It can be used both to identify local damages, determine the causes of their occurrence, but also to conduct a preventive inventory of the technical condition of the operated transport routes.

Further work will be focused on improving the measurement algorithm. The recorded transverse vibrations of the belt come from many phenomena occurring along the entire length of the upper conveyor rod. Faulty cooperation of the belt and the roller is a very complex issue, not related only to the damage to the roller itself. The measurement method should allow to identify all anomalies on the conveyor route, as well as ensure their classification. For this, it is necessary to continue research on real objects with different design and operational parameters. This will provide a sufficient training database for effective detection and classification of roller damage.

Founding

The research work was funded with the research subsidy from the Polish Ministry of Science and Higher Education granted for 2022.

References

1. Ambrożkiewicz B, Syta A, Meier N et al. Radial internal clearance analysis in ball bearings. Eksploatacja i Niezawodnosc – Maintenance and Reliability 2021; 23(1): 42-54, https://doi.org/10.17531/ein.2021.1.5.
2. Ardestani S B. Time Series Anomaly Detection and Uncertainty Estimation using LSTM Autoencoders. 2020.
3. Barros-Daza M J, Luxbacher K D, Lattimer B Y, Hodges J L. Mine conveyor belt fire classification. Journal of Fire Sciences 2021; 40(1): 44-69, https://doi.org/10.1177/07349041211056343.
4. Bartelmus W. Condition monitoring of open cast mining machinery. Wroclaw (Poland), Oficyna Wydawnicza Politechniki Wrocławskiej: 2006.
5. Bartelmus W, Sawicki W. Progress in quality assessment of conveyor idlers. XVI IMEKO World Congress, Vienna (Austria), 2000: 6.
6. Bortnowski P, Kawalec W, Król R, Ozdoba M. Identification of conveyor belt tension with the use of its transverse vibration frequencies. Measurement 2022; 190: 110706, https://doi.org/10.1016/j.measurement.2022.110706.
7. Bortnowski P, Nowak-Szpak A, Król R, Ozdoba M. Analysis and Distribution of Conveyor Belt Noise Sources under Laboratory Conditions. Sustainability 2021; 13(4): 2233, https://doi.org/10.3390/su13042233.
8. Carvalho R, Nascimento R, D'angelo T et al. A UAV-Based Framework for Semi-Automated Thermographic Inspection of Belt Conveyors in the Mining Industry. Sensors 2020; 20(8): 2243, https://doi.org/10.3390/s20082243.
9. Dabek P, Szrek J, Zimroz R, Wodecki J. An Automatic Procedure for Overheated Idler Detection in Belt Conveyors Using Fusion of Infrared and RGB Images Acquired during UGV Robot Inspection. Energies 2022; 15(2): 601, https://doi.org/10.3390/en15020601.
10. Delvecchio S, Bonfiglio P, Pompoli F. Vibro-acoustic condition monitoring of Internal Combustion Engines: A critical review of existing techniques. Mechanical Systems and Signal Processing 2018; 99: 661-683, https://doi.org/10.1016/j.ymssp.2017.06.033.
11. Ding H, Zu J W. Effect of one-way clutch on the nonlinear vibration of belt-drive systems with a continuous belt model. Journal of Sound and Vibration 2013; 332(24): 6472-6487, https://doi.org/10.1016/j.jsv.2013.07.009.
12. Dmitrichenko N F, Milanenko A A, Hluhonets A A, Minyaylo K N. A technique for forecasting the durability of rolling bearings and the optimum choice of lubricants under flood-lubrication and oil-starvation conditions. Journal of Friction and Wear 2017; 38(2): 126-131,

https://doi.org/10.3103/S1068366617020076.
13. Dybała J, Zimroz R. Rolling bearing diagnosing method based on Empirical Mode Decomposition of machine vibration signal. Applied Acoustics 2014; 77: 195-203, https://doi.org/10.1016/j.apacoust.2013.09.001.
14. Dyer D, Stewart R M. Detection of Rolling Element Bearing Damage by Statistical Vibration Analysis. Journal of Mechanical Design 1978; 100(2): 229-235, https://doi.org/10.1115/1.3453905.
15. Faria H D, Lizarralde F, Costa R R et al. ROSI: a mobile robot for inspection of belt conveyor. IFAC-PapersOnLine 2020; 53(2): 10031-10036, https://doi.org/10.1016/j.ifacol.2020.12.2723.
16. Fedorko G, Molnár V, Živčák J et al. Failure analysis of textile rubber conveyor belt damaged by dynamic wear. Engineering Failure Analysis 2013; 28: 103-114, https://doi.org/10.1016/j.engfailanal.2012.10.014.
17. FLEXCO. What Affects Conveyor Roller Life? Technical Solutions for Belt Conveyor Productivity: Factoring Life, Weight, Power, Noise, and Corrosion into Conveyor Roller Performance and Belt Safety. 2020.
18. Gauthier S, Abarzhi S I, Sreenivasan K R et al. Diagnostics of the Technical State of Bearings of Mining Machines Base Assemblies. IOP Conference Series: Materials Science and Engineering 2017; 253(1): 012012, https://doi.org/10.1088/1757-899X/253/1/012012.
19. Gładysiewicz L. Belt conveyors: theory and calculations (in Polish). Wrocław (Poland), Oficyna Wydawnicza Politechniki Wrocławskiej: 2003.
20. Gładysiewicz L, Kawalec W, Król R. Selection of carry idlers spacing of belt conveyor taking into account random stream of transported bulk material. Eksploatacja i Niezawodnosc – Maintenance and Reliability 2016; 18(1): 32-37, https://doi.org/10.17531/ein.2016.1.5.
21. Gunerkar R S, Jalan A K. Classification of Ball Bearing Faults Using Vibro-Acoustic Sensor Data Fusion. Experimental Techniques 2019; 43(5): 635-643, https://doi.org/10.1007/s40799-019-00324-0.
22. Hu Y, Wang L, Wang X et al. Simultaneous measurement of conveyor belt speed and vibration using an electrostatic sensor array. Conference Record - IEEE Instrumentation and Measurement Technology Conference 2015; 2015-July: 757-761, https://doi.org/10.1109/I2MTC.2015.7151363.
23. Kankar P K, Sharma S C, Harsha S P. Fault diagnosis of rolling element bearing using cyclic autocorrelation and wavelet transform. Neurocomputing 2013; 110: 9-17, https://doi.org/10.1016/j.neucom.2012.11.012.
24. Karpiński R, Krakowski P, Jonak J et al. Estimation of differences in selected indices of vibroacoustic signals between healthy and osteoarthritic patellofemoral joints as a potential non-invasive diagnostic tool. Journal of Physics: Conference Series 2021; 2130(1): 012009, https://doi.org/10.1088/1742-6596/2130/1/012009.
25. Kawalec W, Suchorab N, Konieczna-Fuławka M, Król R. Specific Energy Consumption of a Belt Conveyor System in a Continuous Surface Mine. Energies 2020; 13(19): 5214, https://doi.org/10.3390/en13195214.
26. Kirjanów-Błażej A, Jurdziak L, Burduk R, Błażej R. Forecast of the remaining lifetime of steel cord conveyor belts based on regression methods in damage analysis identified by subsequent DiagBelt scans. Engineering Failure Analysis 2019; 100: 119-126, https://doi.org/10.1016/j.engfailanal.2019.02.039.
27. Klein R, Rudyk E, Masad E, Diagnostics R K. Decision and Fusion for Diagnostics of Mechanical Components. Annual Conference of the PHM Society 2011.
28. Krishnan S. Advanced analysis of biomedical signals. Biomedical Signal Analysis for Connected Healthcare 2021: 157-222, https://doi.org/10.1016/B978-0-12-813086-5.00003-7.
29. Król R, Gladysiewicz L, Kaszuba D, Kisielewski W. New Quality Standards of Testing Idlers for Highly Effective Belt Conveyors. IOP Conference Series: Earth and Environmental Science 2017; 95(4): 042055, https://doi.org/10.1088/1755-1315/95/4/042055.
30. Krynke M, Selejdak J, Borkowski S. Diagnosis and damage of bearings. Manufacturing Technology 2012; 12(2): 140-144, https://doi.org/10.21062/ujep/x.2012/a/1213-2489/MT/12/2/140.
31. Liu X. Prediction of belt conveyor idler performance. TRAIL Research School 2016.
32. Liu X, Pang Y, Lodewijks G, He D. Experimental research on condition monitoring of belt conveyor idlers. Measurement 2018; 127: 277-282, https://doi.org/10.1016/j.measurement.2018.04.066.
33. Liu X, Pei D, Lodewijks G et al. Acoustic signal based fault detection on belt conveyor idlers using machine learning. Advanced Powder Technology 2020; 31(7): 2689-2698, https://doi.org/10.1016/j.apt.2020.04.034.
34. Liu Y, Miao C, Li X et al. Research on the fault analysis method of belt conveyor idlers based on sound and thermal infrared image features. Measurement 2021; 186: 110177, https://doi.org/10.1016/j.measurement.2021.110177.
35. Magar S, Narhare T, Gaikwad A, Kapade N. A Review on Improvement of Hydrodynamic Journal Bearing by using Bio-Lubricant. International Journal for Research in Applied Science & Engineering Technology 2021; 9(VI): 1052-1055, https://doi.org/10.22214/ijraset.2021.35162.
36. Miskovic Z, Mitrovic R, Stamenic Z et al. The development and application of the new methodology for conveyor idlers fits testing. Procedia Structural Integrity 2018; 13: 2143-2151, https://doi.org/10.1016/j.prostr.2018.12.150.
37. Morales A S, Aqueveque P, Henriquez J A et al. A technology review of idler condition based monitoring systems for critical overland conveyors in open-pit mining applications. IEEE Xplore 2017: 1-8, https://doi.org/10.1109/IAS.2017.8101839.
38. Nowakowski T, Komorski P. Diagnostics of the drive shaft bearing based on vibrations in the high-frequency range as a part of the vehicle's self-diagnostic system. Eksploatacja i Niezawodnosc – Maintenance and Reliability 2022; 24(1): 70-7, https://doi.org/10.17531/ein.2022.1.9.
39. Olchówka D, Rzeszowska A, Jurdziak L, Błażej R. Statistical Analysis and Neural Network in Detecting Steel Cord Failures in Conveyor Belts. Energies 2021; 14(11): 3081, https://doi.org/10.3390/en14113081.
40. Pariaman H, Luciana G M, Wisyaldin M K, Hisjam M. Anomaly Detection Using LSTM-Autoencoder to Predict Coal Pulverizer Condition on Coal-Fired Power Plant. EVERGREEN Joint Journal of Novel Carbon Resource Sciences & Green Asia Strategy 2021; 9(1): 89-97, https://doi.org/10.5109/4372264.
41. Peruń G, Opasiak T. Assessment of technical state of the belt conveyor rollers with use vibroacoustics methods - preliminary studies. Diagnostyka 2016; 17(1): 75-80.
42. Pihnastyi O, Khodusov V, Kozhevnikov G, Bondarenko T. Analysis of Dynamic Mechanic Belt Stresses of the Magistral Conveyor. Lecture Notes in Mechanical Engineering, Springer Science and Business Media Deutschland GmbH: 2021: 186-195, https://doi.org/10.1007/978-3-030-68014-5_19.
43. Pytlik A, Trela K. Research on tightness loss of belt conveyor's idlers and its impact on the temperature increase of the bearing assemblies.

Journal of Sustainable Mining 2016; 15(2): 57-65, https://doi.org/10.1016/j.jsm.2016.07.001.
44. Qin Z, Chen L, Bao X. Wavelet denoising method for improving detection performance of distributed vibration sensor. IEEE Photonics Technology Letters 2012; 24(7): 542-544, https://doi.org/10.1109/LPT.2011.2182643.
45. Stanik Z. Vibro-acoustic Diagnostics of Rolling Bearings in Vessels. Transactions on Maritime Science 2014; 03(02): 111-118, https://doi.org/10.7225/toms.v03.n02.002.
46. Szrek J, Wodecki J, Błazej R, Zimroz R. An Inspection Robot for Belt Conveyor Maintenance in Underground Mine-Infrared Thermography for Overheated Idlers Detection. Applied Sciences 2020; 10(14): 4984, https://doi.org/10.3390/app10144984.
47. Szurgacz D, Zhironkin S, Vöth S et al. Thermal Imaging Study to Determine the Operational Condition of a Conveyor Belt Drive System Structure. Energies 2021; 14(11): 3258, https://doi.org/10.3390/en14113258.
48. Ursel T, Olinski M. Estimation of objects instantaneous displacement using inertial sensors (in Polish). Interdisciplinary Journal of Engineering Sciences 2019; VII(1): 46-52.
49. Vasić M, Stojanović B, Blagojević M. Failure analysis of idler roller bearings in belt conveyors. Engineering Failure Analysis 2020; 117: 104898, https://doi.org/10.1016/j.engfailanal.2020.104898.
50. Vos K, Peng Z, Jenkins C et al. Vibration-based anomaly detection using LSTM/SVM approaches. Mechanical Systems and Signal Processing 2022; 169: 108752, https://doi.org/10.1016/j.ymssp.2021.108752.
51. Wei Y, Wu W, Liu T, Sun Y. Study of coal mine belt conveyor state on-line monitoring system of based on DTS. Fourth Asia Pacific Optical Sensors Conference 2013; 8924: 89242I, https://doi.org/10.1117/12.2034277.
52. Wodecki J, Michalak A, Zimroz R. Local damage detection based on vibration data analysis in the presence of Gaussian and heavy-tailed impulsive noise. Measurement 2021; 169: 108400, https://doi.org/10.1016/j.measurement.2020.108400.
53. Wodecki J, Zdunek R, Wyłomańska A, Zimroz R. Local fault detectionof rolling element bearing components by spectrogram clustering with Semi-Binary NMF. Diagnostyka 2017; 18(1): 3-8.
54. Zak G, Obuchowski J, Wylomanska A, Zimroz R. Novel 2D representation of vibration for local damage detection. Mining Science 2014; 21: 105-113.
55. Zhao L, Lin Y. Typical Failure Analysis and Processing of Belt Conveyor. Procedia Engineering 2011; 26: 942-946, https://doi.org/10.1016/j.proeng.2011.11.2260.
56. Zimroz P, Shiri H, Wodecki J. Analysis of the vibro-acoustic data from test rig -comparison of acoustic and vibrational methods. IOP Conference Series: Earth and Environmental Science 2021, https://doi.org/10.1088/1755-1315/942/1/012017.
57. Zimroz R, Król R. Failure analysis of belt conveyor systems for condition monitoring purposes. Mining Science 2009; 128(36): 255-270.
58. Wavelet signal denoising - MATLAB wdenoise. [https://www.mathworks.com/help/wavelet/ref/wdenoise.html].
59. 1-D median filtering - MATLAB medfilt1. [https://www.mathworks.com/help/signal/ref/medfilt1.html#description].
60. Butterworth filter design - MATLAB butter. [https://www.mathworks.com/help/signal/ref/butter.html].
61. Condition Monitoring and Prognostics Using Vibration Signals - MATLAB & Simulink. [https://www.mathworks.com/help/predmaint/ug/condition-monitoring-and-prognostics-using-vibration-signals.html].